Materials Research Express

PAPER • **OPEN ACCESS**

Nickel ferrite doped lithium substituted zinc and niobo vanadate glasses: thermal, physical, and electrical characterization

To cite this article: Belay Getachew *et al* 2020 *Mater. Res. Express* **7** 095202

View the article online for updates and enhancements.

You may also like

- Protective Action of Vanadate at Defected Areas of Organic Coatings on Zinc
A. Nazarov, D. Thierry, T. Prosek et al.
- Electrical transport properties of nanocrystalline and bulk nickel ferrite using complex impedance spectroscopy: a comparative study
Sanjeet Kumar Paswan, Lagen Kumar Pradhan, Pawan Kumar et al.
- Magnetic and Dielectric Study of Ceramic Nanocomposite Nickel Ferrite and Barium Titanate Compounds
S. Mahalakshmi, S. Swetha, S. Nithiyanatham et al.

IOP ebooks™

Bringing together innovative digital publishing with leading authors from the global scientific community.

Start exploring the collection–download the first chapter of every title for free.

This content was downloaded from IP address 14.139.128.34 on 16/12/2022 at 09:38

Materials Research Express

PAPER

Nickel ferrite doped lithium substituted zinc and niobo vanadate glasses: thermal, physical, and electrical characterization

Belay Getachew[1], **K P Ramesh**[2] **and Gajanan V Honnavar**[1,3]

[1] Department of Physics, College of Science, Bahir Dar University, 79, Ethiopia
[2] Department of Physics, Indian Institute of Science, Bangalore, 560012, India
[3] On Sabbatical from PES University, Bangalore South Campus, Bangalore, 560100, India

E-mail: gajanan.honnavar@gmail.com

Keywords: zinc and niobo vanadate glasses, DC conductivity, packing density, nickel ferrite, thermal stability

OPEN ACCESS

RECEIVED
28 May 2020

REVISED
14 September 2020

ACCEPTED FOR PUBLICATION
18 September 2020

PUBLISHED
30 September 2020

Original content from this work may be used under the terms of the Creative Commons Attribution 4.0 licence.

Any further distribution of this work must maintain attribution to the author(s) and the title of the work, journal citation and DOI.

Abstract

This study reports a comparison of some thermal, physical, and electrical properties of lithium substituted zinc and niobo vanadate glasses doped with nickel ferrite prepared for the electrical application. These glasses were prepared using the melt quenching technique. Density and differential scanning calorimetry were used to derive various physical and thermal properties. Packing density, the concentration of atoms, separations between atoms were compared between doped and undoped glass families. Thermal stability was estimated and compared. It is found that glasses with 20 mol% of Lithium are more stable than the rest. The thermal stability increases significantly by doping Nickel Ferrite from 5 °C to 30 °C in zinc vanadate glasses. Packing density varies with mol% of lithium ions from 0.43 to 0.42 in zinc vanadate glasses and from 0.40 to 0.42 in niobo vanadate glasses. Doping of Nickel ferrite varies the packing density from 0.42 to 0.43 in zinc vanadate glasses whereas it stabilizes the packing density to 0.42 in niobo vanadate glasses. Out of the two families of glasses, zinc vanadate glass doped with nickel ferrite shows better stability and higher packing density compared with others. DC electrical conductivities of the two families of glasses are almost similar and nickel ferrite doping has a little effect on DC electrical conductivity. Thus it is concluded that the nickel ferrite enhances the stability of the glass while maintaining DC electrical conductivity. This observation is important from the point of view of the electrical application of these glasses.

1. Introduction

Source of renewable energies from solar, wind, biomass, hydropower, geothermal, battery, nuclear plants, etc are day to day demands of this energy-hungry world and the main focus of contemporary research is on the investigation to generate energies for a cleaner and sustainable world [1–6]. Storing energy and using it for different purposes is a crucial aspect. Batteries fall into this category. Recently vanadium-based glasses were used as the cathode material in Li-ion battery [7] and SiO_2 based glasses for 'smart window' [8].

As vanadium can exhibit different oxidation states, it is gaining attention in solid-state chemistry and material science [9, 10]. Transition metal oxide glasses like Vanadate glasses are known to show switching [11], polaronic conduction [12, 13], and ionic conductivity [14]. Polaronic conduction is due to the change of state from V^{4+} to V^{5+} [13], while the ionic conduction is ascribed to the movement of small alkali ions like lithium or sodium.

While investigating cathode material or solid electrolyte for the battery and energy harvesting, it is important to bear in mind that thermal stability is equally important other than good electrical conductivity. The commonly used solid electrolyte in Li-ion battery, $LiCoO_2$, has a disadvantage of losing the thermal stability at high temperatures [15]. Hence there is a need for the investigation of new solid electrolyte materials for energy storage/harvesting and in this communication, an attempt is made to look for the above properties in Zinc and Niobo vanadate glasses and its doped counterparts.

© 2020 The Author(s). Published by IOP Publishing Ltd

Substitution of the atoms with similar atomic size but different valance electronic structures in the glassy matrix brought an important role in improving glass-forming ability [16]. Doping with two or more different metallic ions in the glass is known to increase thermal stability [17]. The effect of the atomic size distribution on glass-forming ability of amorphous metallic alloys has been investigated. It is also found that doping enhances the resistance to crystallize and improves the ability to form a glass [18].

We chose to synthesize binary vanadate glasses with zinc and niobium oxide as co-formers as they widely differ in their valance state and atomic radius. Zinc has a comparable atomic radius with vanadium while Niobium is bigger than both zinc and vanadium. So it is interesting to see the effect of lithium substitution with both zinc and niobium for conductivity as well as stability. Recently Dariush Souri [19] has shown that the addition of Ag_2O to TeO_2-V_2O_5 glasses increases the glass transition temperature and improves the thermal stability of these glasses.

Ferrites have greater thermal stability. Increased ferrite loading in the matrix is known to enhance the thermal stability of the material [20]. Thus in this work, nickel ferrite was chosen as a dopant as it imparts magnetic property along with thermal stability.

In this communication, we present the analysis of the thermal and physical properties of the lithium substituted zinc and niobo vanadate glasses and correlate them to the DC conductivity. We also show that the doping of Nickel Ferrite increases the thermal stability but has a negligible effect on DC conductivity in our glass samples. The novelty of this work is in establishing the fact that the addition of Nickel Ferrite increases the thermal stability while more or less maintain the same electrical conductivity. This is an important observation which may be exploited in the electrical application of these type of glasses. A detailed analysis of electrical conductivity properties derived from Cole-Cole plots, electrical modulus analysis, etc for these glass families will be communicated shortly.

2. Experimental details

2.1. Glass preparation and XRD

Reagent grade chemicals V_2O_5, Nb_2O_5, Li_2CO_3 and ZnO (all from Sigma Aldrich) were used as starting materials to prepare glass samples. In addition to these, Nickel Ferrite ($NiFe_2O_4$) (NF), prepared via combustion technique (using a mixture of Nickel nitrate and Ferric nitrate in ethyl alcohol [21]) was used as dopant. The overall composition of each glass sample is given in table 1. These starting materials were mixed proportionally based on the following formulas: 70 V_2O_5—(30-x) Nb_2O_5—x Li_2O; 70 V_2O_5—(30-x) ZnO—x Li_2O; 68V_2O_5—(30-x) Nb_2O_5– x Li_2O—2 $NiFe_2O_4$ and 68 V_2O_5 - (30-x) ZnO—x Li_2O—2 $NiFe_2O_4$, where x = 15, 20, 25; grounded finely using agate mortar to obtain homogeneous mixing. Batches of nearly 5 g in weight were weighed and taken into a ceramic crucible and heated up to 900 °C–1000 °C for about 80 min with occasional stirring. Then the melt was quenched between brass plates maintained at an elevated temperature of 100 °C to get glasses. These samples were then left to anneal on this plate for about 40 min until the temperature reached an average of 50 °C. The thicknesses of the samples were ranging from 0.5 mm to 0.8 mm.

Powder x-ray diffractometry (XRD) performed on the samples using a Rigaku XRD machine with CuK_α radiation (1.5416 A) and revealed the amorphous nature. A broad hump was seen in the XRD pattern as shown in figure 1. The figure also confirms that the NF used as a dopant has gone into the glass matrix homogeneously and has not created any clusters of its own as no sharp crystalline peaks were observed in the pattern.

2.2. Physical property and thermal characterization:

Density of the prepared glasses were determined using the Archimedes principle, to an accuracy of ± 0.004 g cc^{-1}. Xylene was used as an immersion liquid with a density of 0.864 g cc^{-1} (declared by the manufacturer). A high resolution electronic weighing balance (with an accuracy of 0.0001 g) was used to measure the weights of the samples in air and liquid. The molar volume was calculated using the equation $V_m = \frac{M}{\rho}$, where M is the molecular weight of the glass sample, which was calculated as $M = \sum x_i w_i$, where x_i and w_i are the mole fraction and molecular weight of the component i and ρ is the density, respectively.

The thermal behaviors of the prepared glasses were recorded using Differential Scanning Calorimeter (DSC) (TA Instruments) at a heating rate of 10 K per minute. DSC curves of all glasses with and without doping are shown in figure 2. The glass transition T_g and onset of crystallization temperature T_x (to an accuracy of ± 0.05 °C) were determined from these curves.

2.3. DC electrical conductivity measurements

A 5 mm diameter mask was used to paint high purity conducting silver (SPI supplies, USA) contact. The real and Imaginary part of the complex impedance was measured using Agilent Precision Impedance Analyzer 4194A over the frequency range of 100 Hz to 10 MHz with an oscillator level of 500 mV which was found to be well

Table 1. Glass content in mol%, glass transition temperature (T_g), onset crystallization (T_x), thermal stability (S), density, molar volume, and Packing density.

		Glass content (mol %)										
S.No	Sample Code	V_2O_5	ZnO	Nb_2O_5	Li_2O	$NiFe_2O_4$	T_g (°C)	T_x (°C)	$S = T_x$-T_g (°C)	Density (g cc^{-1})	Molar Volume (cc)	Packing Density
1	VZL 15	70	15	0	15	0	236	242	6	2.999	4801.570	0.428
2	VZL 20	70	10	0	20	0	233	253	20	2.938	4814.563	0.426
3	VZL 25	70	5	0	25	0	238	248	10	2.867	4842.765	0.422
4	VZLFe 15	68	15	0	15	2	238	270	32	3.108	4832.394	0.424
5	VZLFe 20	68	10	0	20	2	235	270	35	3.024	4761.168	0.429
6	VZLFe 25	68	5	0	25	2	228	253	25	2.962	4732.333	0.430
7	VNL 15	70	0	15	15	0	236	254	18	2.863	5996.775	0.396
8	VNL 20	70	0	10	20	0	252	291	39	2.932	5453.635	0.414
9	VNL 25	70	0	5	25	0	238	262	24	2.888	5127.139	0.419
10	VNLFe 15	68	0	15	15	2	261	325	64	3.108	5557.444	0.425
11	VNLFe 20	68	0	10	20	2	265	311	46	3.04	5321.541	0.423
12	VNLFe 25	68	0	5	25	2	249	281	32	2.962	5034.673	0.425

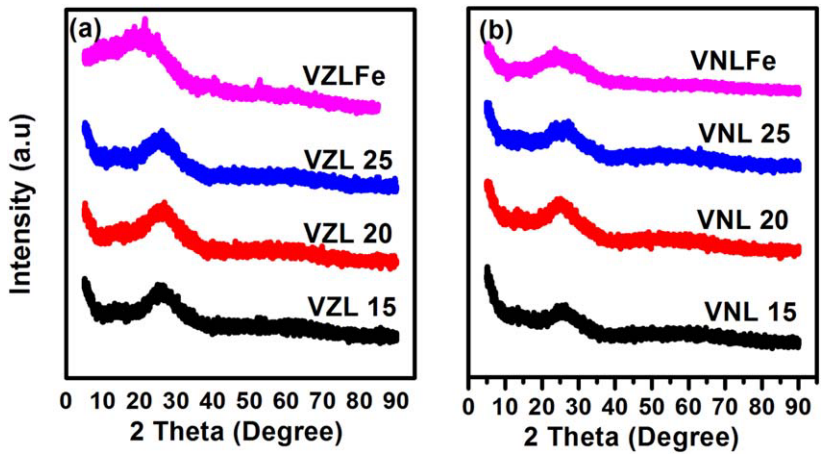

Figure 1. XRD patterns of undoped and doped glasses with Nickel ferrite (a) VZL and VZLFe (b) VNL and VNLFe.

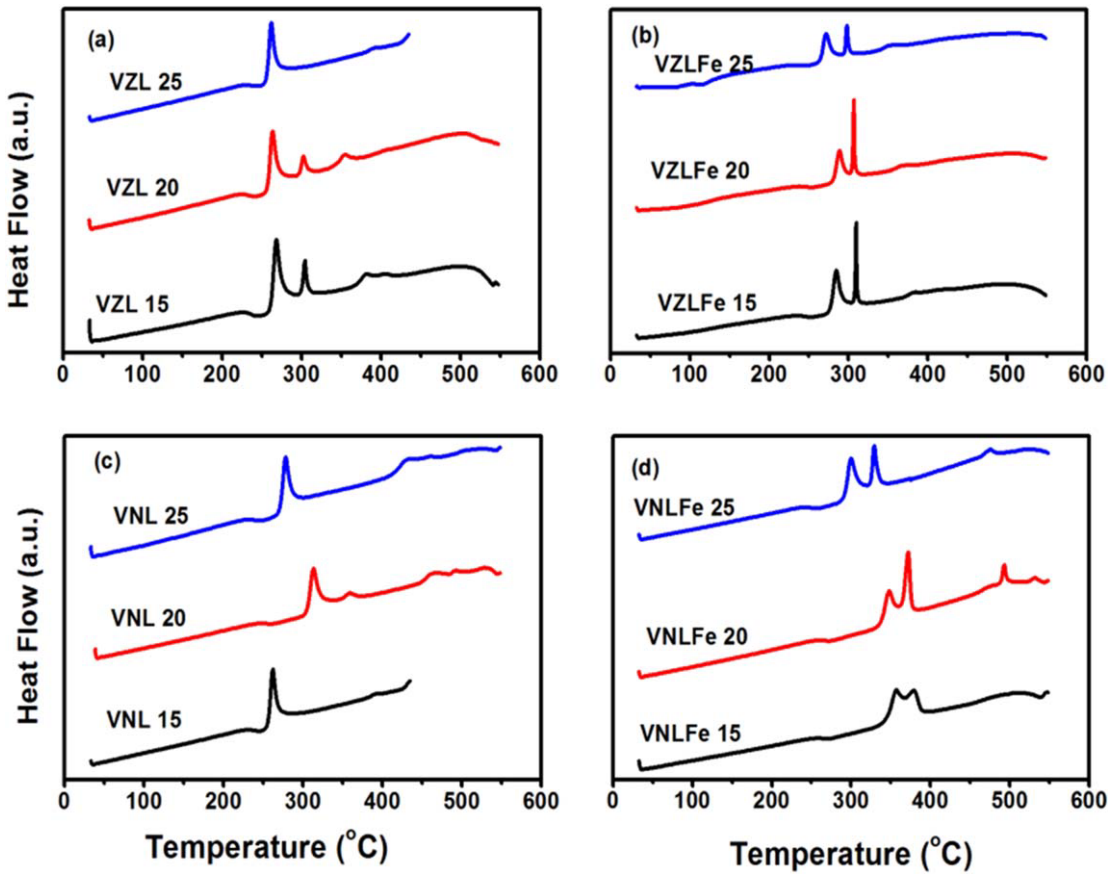

Figure 2. DSC Patterns of doped and undoped glass samples (a) VZL (b) NF doped VZL (c) VNL (d) NF doped VNL.

within the linear response limit. Temperature-dependent measurements were performed using a home built furnace with a temperature controller in the range 120 °C to 300 °C; the temperature was measured using a K type thermocouple to an accuracy of ±1 °C. Complex conductivity $\hat{\sigma} = \frac{k}{\hat{Z}(f)}$, where $\hat{Z}(f)$ - complex impedance measured from the impedance analyzer, k—cell constant given by d/A(d is the thickness and A is the area of cross-section of the sample) [22] was calculated for each sample and for all the temperature range from 120 °C to 300 °C. We report here only the analysis of the frequency-independent DC part of the conductivity data.

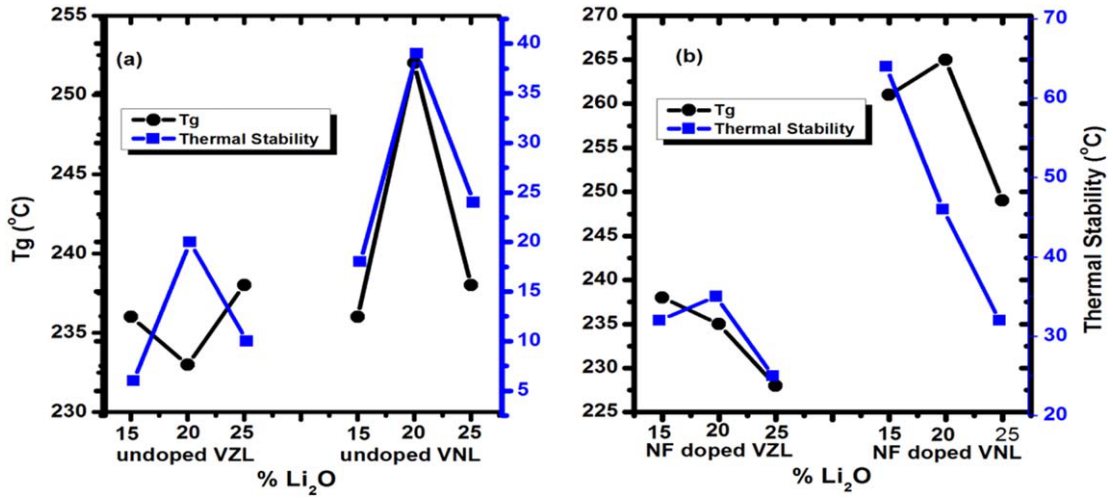

Figure 3. Glass transition temperature and thermal stability of Glass samples (a) undoped VZL and VNL (b) NF doped VZL and VNL samples as regards % Li_2O.

3. Results and discussion

3.1. Thermal properties

The thermal stability S of the glasses against crystallization was calculated by the equation:

$$S = T_X - T_g \tag{1}$$

where, T_X and T_g are the onset of crystallization temperature and the glass transition temperature, respectively. The values of the glass transition temperature, T_g, the onset of crystallization temperature, T_x and thermal stability S, are listed in table 1. The compositional dependence of the glass transition temperature T_g and thermal stability S of the glass samples are plotted in figure 3 in accordance with mol%Li_2O for undoped and NF doped glasses.

In figure 3(a) a comparison of T_g and S for VZL and VNL glass samples are made. T_g and S have an opposite trend with respect to each other in VZL samples whereas in VNL samples these properties scale one with the other. The VZL and VNL samples doped with NF have shown an almost linear variation of these properties.

3.2. Density, molar volume, and packing density

Density is used to determine various structural aspects of glasses [23]. The same family of glass samples may be differing in density because of the difference in packing and amount of constituents. It depends on the nature and how ions can enter the glass structure [24]. Packing density is an inherent property of glass. In the present glasses, there may be ionic and covalent packing.

Table 1 contains the calculated density values, molar volume, and packing factor for undoped and NF doped glasses. Hoppe suggested that the packing fraction may be more useful to express the experimental density of glasses even more than molar volume because the packing fraction is helpful in revealing the microscopic structure of the glass. He pointed out that packing is inherently limited by the choice of ionic radii, which have a larger impact on volume [25].

The glass sample having a component $x\%A_yB_z$, where A is a cation, B is an anion and x is mol%, y and z are the valencies of the cation and anion, respectively. Then the packing factor V_p is given by

$$V_p = \frac{4\pi N}{3}(yr_A^3 + zr_B^3) \tag{2}$$

where, N is the Avogadro number, r_A and r_B are the ionic radii of the cation and anion, respectively.[OE]

10.1088/0034-4885/72/4/046501Consequently, the packing density V_d is calculated by

$$V_d = \frac{\rho}{M}\sum x_i V_p \tag{3}$$

where ρ and M are density and its molecular weight, respectively.

Figure 4 shows the variation of density and packing density with respect to variation in lithium content in undoped and doped glasses.

The packing density of the undoped glass samples is less than their doped counterparts. The packing density of undoped VZL is greater than the undoped VNL glass sample (see figure 4(a)). From figure 4(b), one can

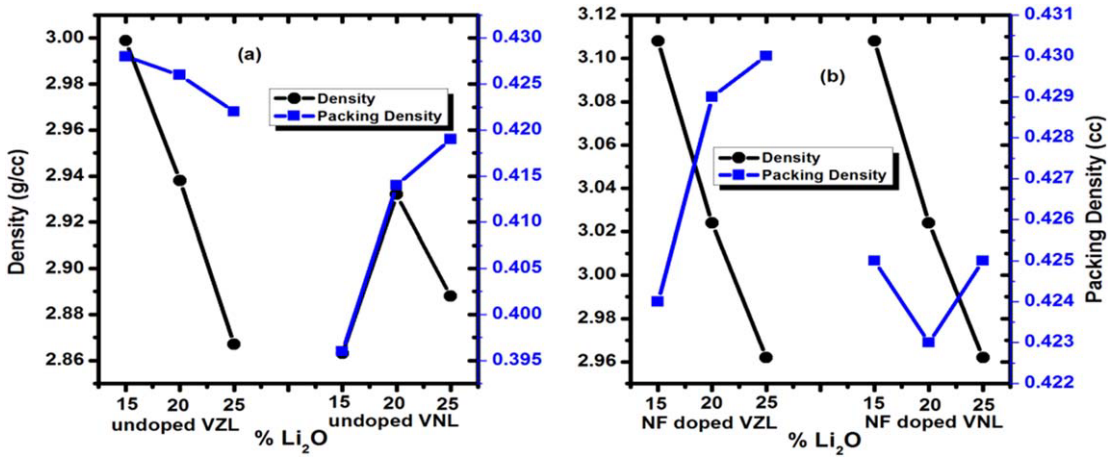

Figure 4. Variation of Density and Packing density in glass samples (a) undoped VZL and VNL (b) NF doped VZL and VNL with respect to % Li_2O.

observe that in the case of NF doped VZL and VNL, packing density in VZLFe increases monotonically with the lithium content whereas it goes through a minimum in VNLFe as lithium content increases.10.1088/0034-4885/72/4/04650110.1088/0034-4885/72/4/046501

3.3. Concentration and distance of separation between atoms

The concentration of ions A and B in the general formula $x\%A_bB_c$ is given by the following relation:

$$n(A) = \frac{\text{bxN}}{100V_m} \tag{4}$$

10.1088/0034-4885/72/4/046501and for ion B it is given by

$$n(B) = \frac{\text{cxN}}{100V_m} \tag{5}$$

where, x, N and V_m are mole percentage, Avogadro number, and molar volume, respectively.

From values of concentration of atoms, the average shortest distance of separation between like atoms can be calculated using the relation:

$$r = \left(\frac{1}{n}\right)^{\frac{1}{3}} \tag{6}$$

Using equations (4)–(6), the concentrations of Vanadium n(V) and Oxygen n(O), the separation between V atoms r(V–V) and O atoms r(O–O) are calculated. The values are listed in table 2. The average shortest separation between V and O, r(V–O) for VO^5 configuration is calculated by considering vanadium to be at the center of square made up of four oxygen atoms. There will be one oxygen connected to vanadium on top. For simplicity, all oxygen vanadium distances are considered to be the same. As can be seen from table 2, the values of r(V-V) for VZL of undoped glasses lie between 1.78 nm and 1.79 nm, VNL undoped glasses lie between 1.923 nm and 1.825 nm. For VO^{5+}, r(V-O) for VZL lies from 4.65 Å to 4.66 Å and VNL from 4.99 Å to 4.74 Å. This shows that in VZL glasses the V—O distance is unaffected by the lithium substitution. But in VNL glasses the substitution of lithium has an effect of slightly decreasing the V—O distance.

The concentration of vanadium ions n(V) for VZL and VNL is from (~1.76 to 1.74) $\times 10^{+20}$/cc and (~1.41 to 1.64) $\times 10^{+20}$/cc, respectively. Slight increase of r(V-V) and r(V-O) in the VZL family of glasses (doped and undoped) with the increase of lithium oxide indicates that when lithium ions are added, the structure of the glass opens up as well as weakens. Therefore, the T_g decreases. Similarly, the decrease of r(V-V) and r(V-O) for VNL glasses (doped and undoped) as the lithium mol% increases shows that the structure becomes compact and the glass strengthens. Thus the glass transition temperature T_g increases. This may be because the atomic radium of Zn (138 pm) is smaller than that of Nb (146 pm) which has comparable atomic radium as that of Li (145 pm). As Zn is replaced by larger Li, the network opens up in the case of VZL glasses. In the case of VNL where the atomic radii of Nb and Li are comparable, the electropositivity of Li may prevail. As Li is more electropositive than Nb (electronegativity 0.98 as compared to Nb with electronegativity 1.6), the substitution of the former at the expense of the later breaks the oxygen bonds and creates more non-bridging oxygen. This collapses the glass network.

Table 2. Concentration of ions, atom-atom separation and stretching force constant between atoms of glass samples. The values are derived from the molar volume which is calculated using density values accurate to 3rd decimal. Thus the 3rd decimal place is retained for all the derived values in the table.

Sample Code	n(V) x10^{+20}/cc	n(O) x10^{+20}/cc	r(V-V) (nm)	r(O-O) (nm)	r(V-O) VO^5 (Å)
VZL15	1.756	1.786	1.786	1.316	4.654
VZL20	1.751	1.787	1.787	1.317	4.658
VZL25	1.741	1.791	1.791	1.320	4.666
VZLFe 15	1.695	1.807	1.807	1.331	4.705
VZLFe 20	1.720	1.798	1.798	1.325	4.683
VZLFe 25	1.731	1.795	1.795	1.322	4.674
VNL15	1.406	1.923	1.923	1.417	4.987
VNL20	1.546	1.863	1.863	1.373	4.824
VNL25	1.644	1.825	1.825	1.345	4.735
VNLFe 15	1.474	1.893	1.893	1.395	4.934
VNLFe 20	1.539	1.866	1.866	1.375	4.862
VNLFe 25	1.627	1.832	1.832	1.350	4.774

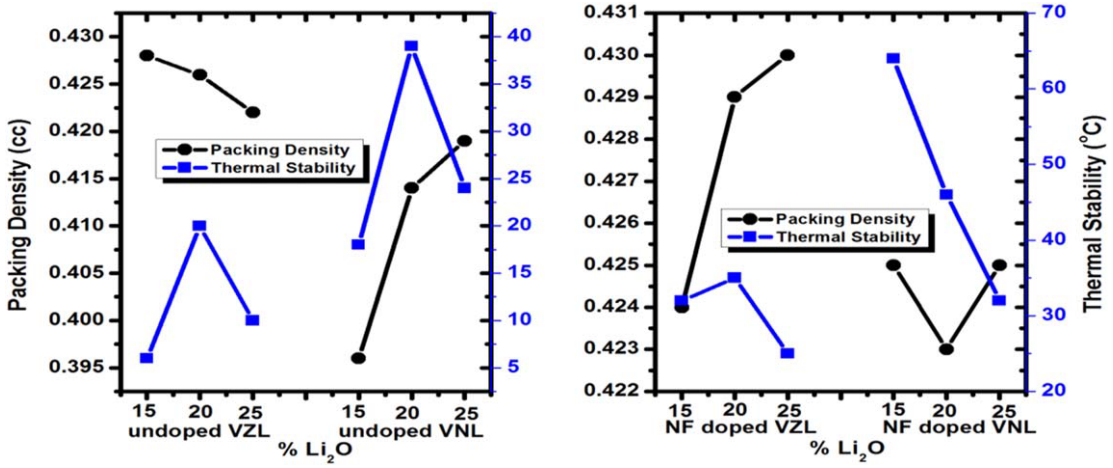

Figure 5. Packing density and Stability of glass samples (a) VZL and VNL (b) NF doped VZL and VNL with respect to %Li_2O.

From figure 5, we observe that as the packing density of the glasses varies, it affects the thermal stability. Here the concentration of lithium ions is also significant in addition to the nickel ferrite. The VNL families of glasses are less packed compared to the VZL family of glasses.

The doped glasses have good thermal stability. A larger value of thermal stability may be needed for the crystallization of different phases inside the glass. Doping nickel ferrite has not only increased the thermal stability and packing density of the glass sample but it has also become the cause for more than one exothermic peaks to be formed up to the temperature we have run the DSC measurements. The presence of more than one peaks shows that different phases could be crystallized in the glass.

From all the corroborative studies performed on the VNL and VZL family of glasses, we have found that the addition of Nickel Ferrite greatly increases the thermal stability of these glasses. This may be of technological importance as higher thermally stabilized glasses are more useful in industry. Among VNL and VZL family, VZL is thermally more stable and have higher packing density.

3.4. DC electrical conductivity

The DC conduction is glasses can be due to polaron hopping or ionic motion or sometimes both/mixed. Moving ions carry a charge and thus produce an electrical response that can be detected by a variety of experimental techniques [26]. There are experimental facts that in materials with high ion concentration, at any given time only part of the ions are actively involved in a back-and-forth motion and become the cause for conduction [27, 28]. Information about these motions on different time and length scales can be obtained by using impedance or conductivity spectroscopy.

The total conductivity obeys Joncher's power law. The real part of the frequency-dependent conductivity has a relation:

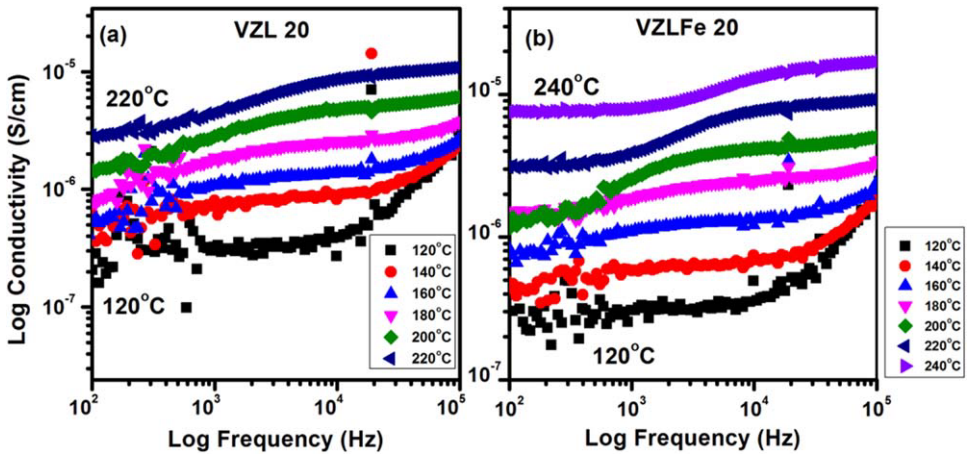

Figure 6. Representative conductivity spectra of (a) VZL 20 and (b) VZLFe 20. The plots are for different temperatures as shown. Space charge (Electrode) polarization can be observed at low frequencies. Data was noisy below 100 Hz.

Table 3. DC conductivity values of the present glass samples at different temperatures.

	DC Conductivity (S cm^{-1}) at				
Sample Code	120 °C	140 °C	160 °C	180 °C	220 °C
VZL 15	3.47×10^{-7}	1.08×10^{-6}	1.95×10^{-6}	3.67×10^{-6}	1.7×10^{-6}
VZL 20	3.2×10^{-7}	8.61×10^{-7}	1.33×10^{-6}	2.47×10^{-6}	4.14×10^{-6}
VZL 25	6.24×10^{-7}	1.55×10^{-6}	2.92×10^{-6}	5.68×10^{-6}	1.37×10^{-5}
VZLFe 15	3.35×10^{-7}	9.45×10^{-7}	1.89×10^{-6}	3.12×10^{-6}	1.70×10^{-6}
VZLFe 20	2.76×10^{-7}	7.03×10^{-7}	1.38×10^{-6}	2.57×10^{-6}	3.5×10^{-6}
VZLFe 25	2.52×10^{-7}	6.36×10^{-7}	1.29×10^{-6}	2.62×10^{-6}	1.67×10^{-6}
VNL 15	2.2×10^{-6}	6.66×10^{-6}	1.21×10^{-5}	2.1×10^{-5}	4.54×10^{-5}
VNL 20	7.67×10^{-7}	2.0×10^{-6}	3.12×10^{-6}	3.76×10^{-6}	3.07×10^{-6}
VNL 25	6.28×10^{-7}	1.78×10^{-6}	3.17×10^{-6}	3.65×10^{-6}	1.62×10^{-6}
					(5.22×10^{-6})[a]
VNLFe 15	4.27×10^{-6}	1.23×10^{-5}	2.1×10^{-5}	3.46×10^{-5}	(6.47×10^{-5})[a]
VNLFe 20	4.79×10^{-7}	1.19×10^{-6}	2.29×10^{-6}	4.73×10^{-6}	2.06×10^{-6}
VNLFe 25	3.37×10^{-7}	1.10×10^{-6}	2.17×10^{-6}	4.25×10^{-6}	(1.04×10^{-5})[a]

[a] Estimated Value.

$$\sigma'(\omega) = \sigma_o\left[1 + \left(\frac{\omega}{\omega_o}\right)^n\right] \tag{8}$$

Where, $\sigma'(\omega)$ and σ_o are AC and DC conductivities. ω_o is the threshold or onset frequency above which the AC contribution takes over and n is the dimensionless frequency exponent dependent on temperature [29].

Figure 6 shows the conductivity spectra of representative glass samples. The DC conductivity was extracted by extrapolating the frequency-independent region of the spectra. In the figure, the spectra are shown from 100 Hz to 10 KHz. Data lower than 100 Hz was noisy and after 10 KHz the frequency dependency of conductivity sets in. Table 3 lists the DC conductivity values at different temperatures for all the glass samples.

A closer look at table 3 reveals that the doping of Nickel ferrite has not enhanced the conductivity to a large extent. But the doping is found to increase the thermal stability of these glasses.

Figure 7 presents the variation in DC conductivity as a function of packing density at various temperatures. In figures 7(a)–(c) it is observed that the packing density decreases slightly in case of undoped and increases in case of doped VZL glasses as lithium is added. The DC conductivity is seen to decrease first and then increase as the lithium content increases in VZL glasses while the doped VZL glasses (VZLFe) show a monotonic decrease in conductivity with respect to increase in packing density. But at temperature 220 °C, glass with 20 mol% lithium content shows highest conductivity.

It is observed that in VNL family of glasses DC conductivity decreases as packing density increases as a function of lithium concentration. An increasing temperature slightly changes the behavior of 25 mol% lithium glass; otherwise, both doped and undoped glasses have a similar trend of decreasing conductivity with an increase in packing density (see figures 7(d)–(f)).

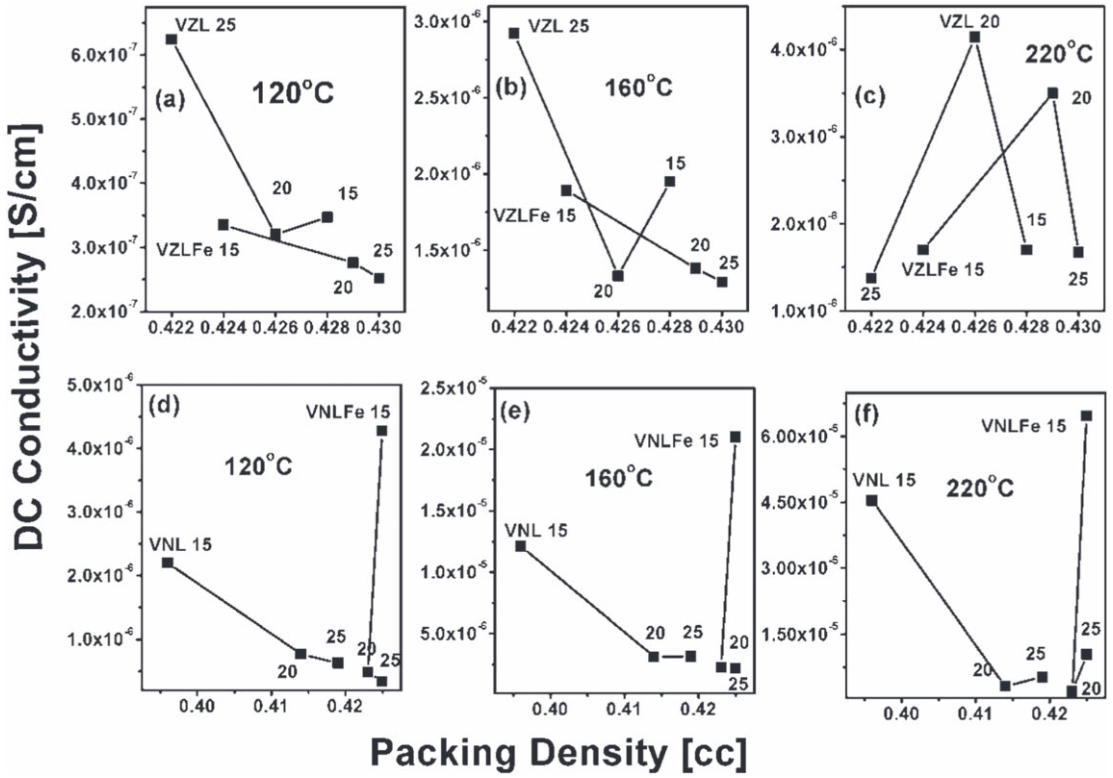

Figure 7. DC conductivity at 120, 160 and 220°C versus packing density: (a)–(c) VZL and VZLFe. (d)–(f) VNL and VNLFe. Numbers 15, 20 and 25 in line with their glass families are mol% Li_2O.

A decrease in packing density represents more open space and lower hindrance to the movement of the mobile ions responsible for electrical conduction. Thus even though the variation in packing density is very small there is a change in conductivity in VZL and VZLFe glasses.

On the other hand, a gradual increase in packing density in VNL and VNLFe glasses hinders the movement of the mobile ions resulting in a monotonic decrease in conductivity.

4. Conclusion

In the present study, the thermal, physical, and DC electrical properties of lithium substituted zinc and niobo vanadate glass samples were investigated especially paying attention to the impact of doping nickel ferrite. XRD, Density, and DSC measurements were carried out. Physical and thermal properties like packing density, the distance between atoms, the concentration of species, thermal stability were derived from these measurements. The thermal stability increases significantly by doping Nickel Ferrite from 5 °C to 30 °C in zinc vanadate glasses. Packing density varies with mol% of lithium ions from 0.43 to 0.42 in zinc vanadate glasses and from 0.40 to 0.42 in nickel vanadate glasses. Doping of Nickel ferrite varies the packing density from 0.42 to 0.43 in zinc vanadate glasses whereas it stabilizes the packing density to 0.42 in nickel vanadate glasses. The variation of density of cross-linking, the tightness of the packing in the network, the coordination of the network formers are the causes for variation of densities, molar volume and packing density of the glass samples. The change of atomic sizes and electronegativity within the composition were also playing a great role in the thermal and structural changes of the glass samples. It is found that lithium substituted zinc vanadate glasses and its doped counterparts are more thermally stable than the niobo vanadate glasses. Due to coordination change in the glass systems as temperature varies, DC conductivity of glass shows anomalous behavior.

Acknowledgments

BG wholeheartedly acknowledges the financial support extended by Bahir Dar University to cover the travel and living expenses while visiting the Indian Institute of Science for performing research. The authors would like to greatly acknowledge the help in density measurements by Dr. Brian Jeevan Fernandes and Dr. K Ramesh. The

authors also would like to acknowledge the central facility at the Department of Physics, IISc, Bangalore, India for the measurement of DSC, XRD, and impedance measurements.

Authors contributions

GVH and KPR formulated the research, KPR provided the facilities to carry out the research. BG performed the experiments and collected the data, BG and GVH analyzed the data. All the authors contributed to the manuscript.

ORCID iDs

Belay Getachew https://orcid.org/0000-0002-1718-5481
Gajanan V Honnavar https://orcid.org/0000-0002-6287-4366

References

[1] You J, Dou L, Hong Z, Li G and Yang Y 2013 *Prog. Polym. Sci.* **38** 1909
[2] Dresselhaus M S and Thomas I L 2001 *Nature* **414** 332
[3] Rashid S M, Deb B and Gupta R 2018 *AIP Conf. Proc.* **1998** 020017
[4] Akia M, Yazdani F, Motaee E, Han D and Arandiyan H 2014 *Biofuel Res. J* **1** 16
[5] Mohan D, Pittan C U Jr and Steele P H 2006 *Energy Fuels* **20** 848
[6] Long J W, Dunn B, Rolison D R and White H S 2004 *Chem. Rev.* **104** 4463
[7] Ayfon S, Krumeich F, Mensing C, Borgschulte A and Nesper R 2014 *Sci. Rep.* **4** 7113
[8] Ke Y, Balin I, Wang N, Lu Q, Tok A I, White T J, Magdassi S, Abdulhalim I and Long Y 2016 *ACS Appl. Mater. Interfaces* **8** 33112
[9] Qu Q, Zhu Y, Gao X and Wu Y 2012 *Adv. Energy Mater.* **2** 950
[10] Li Y, Yao J, Uchaker E, Yang J, Huang Y, Zhang M and Cao G 2013 *Adv. Energy Mater.* **3** 1171
[11] Mansour E, Moustafa Y M, El-Damrawi G M, Abd El-Maksoud S and Doweidar H 2001 *Physica* B **305** 242
[12] Austin I G and Sayer M 1974 *J. Phys. C: Solid State Physics* **7** 905
[13] Owen A E 1977 *J. Non-Cryst. Solids* **25** 370
[14] Ungureanu M C, Lévy M and Souquet J L 2000 *Ceramics—Silikáty* **44** 81
[15] Nitta N, Wu F, Taelee J and Yushin G 2015 *Mater. Today* **18** 252
[16] Inoue A, Zhang T and Masumoto T 1990 *Mater. Trans., JIM* **31** 177
[17] Bingham P A, Hand R J and Forder S D 2006 *Mater. Res. Bull.* **41** 1622
[18] Pisarski W A, Goryczk T, Wodecka-Dus B, Płonska M and Pisarska J 2005 *Mat. Sci. Eng. B—Adv* **122** 94
[19] Souri D 2017 *J. Non-Cryst. Solids* **475** 136
[20] Flaifel M H, Ahmad S H, Hassan A, Bahri S, Tarawneh M A and Yu L 2013 *Composites: Part* B **52** 334
[21] Sivakumar P, Ramesh R, Ramanand A, Ponusamy S and Muthamizhcheivan C 2011 *Mater. Res. Bull.* **46** 2208
[22] Roling B 1999 *J. Non-Cryst. Solids* **244** 34
[23] Charles R J 1958 *J. Appl. Phys.* **29** 1549
[24] Doweidar H 1998 *J. Non-Cryst. Solids* **240** 55
[25] Hoppe U 1999 *J. Non-Cryst. Solids* **248** 11
[26] Dyre J C, Maass P, Roling B and Sidebottom D L 2009 *Rep.Prog.Phys* **72** 046501
[27] Roling B, Martiny C and Bruckner S 2001 *Phys. Rev.* **63** 214203
[28] Murugavel S and Roling B 2004 *J. Phys. Chem.* B **108** 2564
[29] Almond D P and West A R 1983 *Nature (London)* **306** 456